

# Direct numerical simulations of 2D channel flows in the presence of polymers

Y. L. XIONG<sup>1</sup>, C. H. BRUNEAU<sup>1</sup> and H. KELLAY<sup>2</sup>

<sup>1</sup> *Université Bordeaux 1, Institut de Mathématiques de Bordeaux, INRIA Team MC2, CNRS UMR 5251 351 cours de la Libération, 33405 Talence, France, EU*

<sup>2</sup> *Université Bordeaux 1, Laboratoire Ondes et Matière d'Aquitaine, UMR 5798 CNRS - 351 cours de la Libération, 33405 Talence, France, EU*

received 11 February 2011; accepted in final form 27 July 2011  
published online 1 September 2011

PACS 47.27.-i – Turbulent flows  
PACS 47.27.E- – Turbulence simulation and modeling  
PACS 47.50.-d – Non-Newtonian fluid flows

**Abstract** – Direct numerical simulations of a two-dimensional channel flow in the presence of a polymeric fluid are presented. The flow is perturbed by an array of cylinders which generates a turbulent flow downstream and whose statistical properties are studied in detail. Several features emerge from this study such as the reduction of turbulent fluctuations at large scales, the reduction of the energy transfer rate, and the reduction of the fluctuations of the enstrophy and energy transfer rates. These features are in excellent agreement with previous experimental measurements and show that despite the possible limitations of the model used to describe the polymeric fluid (an Oldroyd-B model), the changes observed here and in experiments may be generic to two-dimensional turbulent flows. An examination of the stress and elongation fields shows that the stresses are important in strong elongation zones pointing out that the effects due to polymers may have their origin in the large elongation zones which develop between vortices.

Copyright © EPLA, 2011

The influence of minute amounts of polymer on turbulent flows can be dramatic [1–3]. The decrease of the turbulent drag in pipes, for example, can reach nearly 80% upon the addition of a few parts per million by weight of long-chain flexible polymers. This effect has been studied in three-dimensional pipes for obvious reasons and has, more recently, been tackled in quasi-two-dimensional flows using soap films [4,5]. For the two-dimensional case, an intriguing effect has been observed experimentally. Indeed, and for very small amounts of polymer, the statistics of the velocity fluctuations were affected primarily at the large-scale end, leaving the small scales almost untouched [4]. It was suggested that the polymers may affect the mechanisms leading to the inverse cascade of energy, a special feature of two-dimensional turbulent flows. This non-trivial effect has later been confirmed by numerical work which also suggested that polymers may also affect the spectrum of Lyapunov exponents of such flows [6]. Experimentally, this latter effect has been attributed to the reduction in the fluctuations of the enstrophy transfer rate. The picture so far is that the polymers affect the energy injection rate from the small to the large scales

and affect the fluctuations in the enstrophy transfer rate. These features make the two-dimensional case an excellent test bed for studying the interaction between polymers and a turbulent flow, an issue of tremendous fundamental and practical interest [1,7].

We here focus on direct numerical simulations of a two-dimensional channel flow perturbed by an array of cylinders for the case of an Oldroyd-B fluid. This type of non-Newtonian fluid displays no shear thinning and is therefore a purely elastic fluid. The use of the channel geometry is similar to that used in experiments so that our simulations may be compared directly to soap film experiments in the presence of polymers [4]. It is our aim here to first test the validity of previous observations but in a purely two-dimensional case and, further, to measure quantities difficult to access experimentally such as the elastic stress and its correlation to flow properties such as the elongation field, for example.

The dynamics examined here is that of an incompressible two-dimensional viscoelastic Oldroyd-B constitutive fluid described by the non-dimensional equations detailed below. A penalization scheme is used to represent the solid

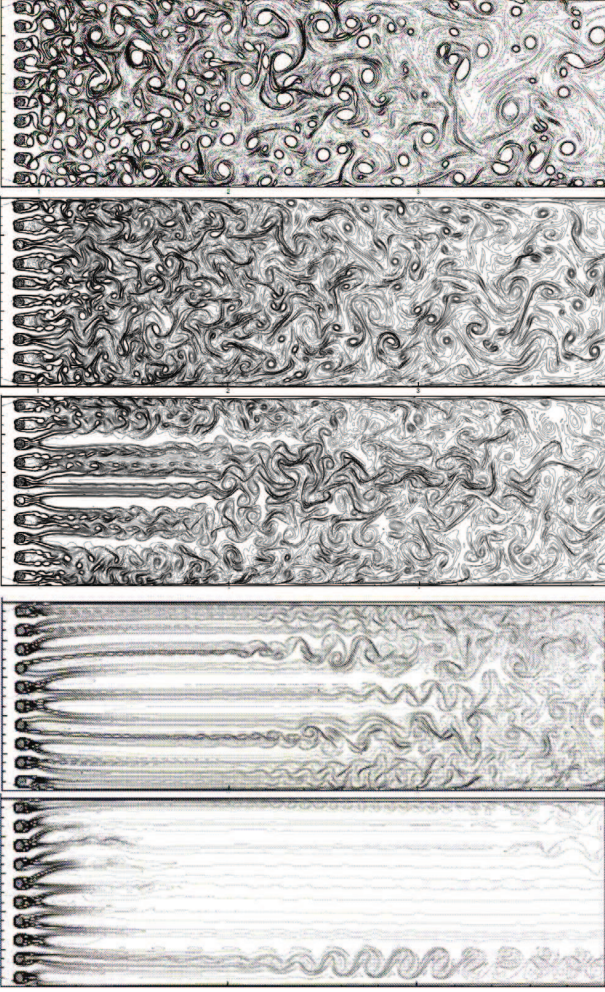


Fig. 1: Snapshot of the vorticity fields for different Weissenberg numbers (from top to bottom:  $Wi = 0, 2, 3, 4,$  and  $6$  for case 2). As  $Wi$  increases we note that the appearance of vortical structures occurs even further from the array of cylinders in such a way that for  $Wi = 6$ , the length of the channel becomes too small to observe them. They are, however, still visible near the walls.

bodies (the cylinders) on a Cartesian mesh of the domain whose length is 4 times its width. Here the coordinate  $x$  denotes the streamwise direction and  $y$  denotes the direction transverse to the flow. The simulated domain is  $0 \leq x \leq 4$  and  $0 \leq y \leq 1$ . The equations simulated here read

$$\begin{aligned} \nabla \cdot \mathbf{u} &= 0 \\ \partial_t \mathbf{u} + (\mathbf{u} \cdot \nabla) \mathbf{u} + \frac{\mathbf{u}}{K} &= -\nabla p + \frac{1}{Re} \left[ (1 - \beta) \Delta \mathbf{u} + \frac{\beta}{Wi} \nabla \cdot \boldsymbol{\sigma} \right] \\ \partial_t \boldsymbol{\sigma} + (\mathbf{u} \cdot \nabla) \boldsymbol{\sigma} + \frac{\boldsymbol{\sigma}}{K} + \frac{\boldsymbol{\sigma} - \mathbf{I}}{Wi} &= (\nabla \mathbf{u}) \cdot \boldsymbol{\sigma} + \boldsymbol{\sigma} \cdot (\nabla \mathbf{u})^T + \kappa \Delta \boldsymbol{\sigma}, \end{aligned}$$

where  $\mathbf{u}$  is the two-dimensional velocity vector,  $p$  is the pressure,  $\boldsymbol{\sigma}$  is the conformation tensor of polymer molecules, their elongation is measured by its trace. The

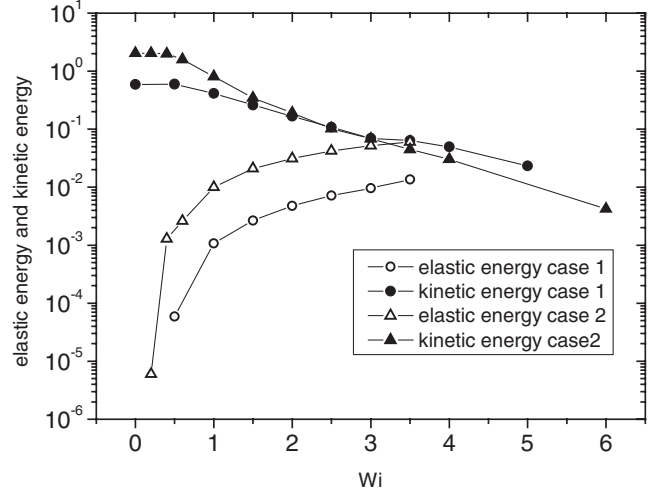


Fig. 2: Kinetic and elastic energy for the two configurations used *vs.*  $Wi$  at point  $x = 3.8$  and  $y = 0.4$ . Note that for  $Wi = 6$ , the small value of the fluctuations is due to the fact that vortical structures have been suppressed even far from the array.

parameter  $K$  is the non-dimensional permeability coefficient used in the penalization term; it is set to  $10^{16}$  in the fluid zone to recover the genuine equations and to  $10^{-7}$  in the solid cylinders to enforce  $\mathbf{u}$  and  $\boldsymbol{\sigma}$  to vanish [8]. Penalizing the tensor is not necessary but it appears that doing so leads to better numerical stability. The quantity  $(1 - \beta)$  denotes the ratio of the solvent viscosity to the viscosity of the polymer solution, it is set to 0.99 in our simulations. The term  $\kappa \Delta \boldsymbol{\sigma}$  is an artificial diffusive term to prevent numerical instabilities,  $\kappa$  is taken small enough ( $10^{-3}$ ) to not affect the solution significantly in this study [9]. The Reynolds number  $Re$  and the Weissenberg number  $Wi$  are non-dimensionalized by the same referenced velocity and length. In our results,  $Re$  and  $Wi$  are defined by  $Re = UR/\eta$  and  $Wi = \tau U/R$ , respectively, where  $U$  is the mean velocity of the inlet Poiseuille flow,  $R = 0.025$  is the radius of the cylinders used and which are located as an array in the transverse direction of the channel at one width from the entrance. Here  $\eta$  and  $\tau$  are, respectively, the viscosity and the relaxation time of the polymer solutions. The numerical simulations are carried out by a multigrid method with a  $2048 \times 512$  fine grid and a finite differences approximation [10]. This numerical scheme has been shown to give excellent agreement with experimental measurements of two-dimensional flows in the turbulent state [11]. It should be noted that the choice of the Oldroyd-B model is dictated by its simplicity despite the fact that it has limitations [12]. This model has also been shown to display several features observed in experiments such as drag reduction and elastic turbulence [13]. A more recent study of ours [14] showed important modifications of the wake behind a cylinder: the drag on a single cylinder can exhibit both enhancement and reduction, as seen in experiments [15,16], and the phase

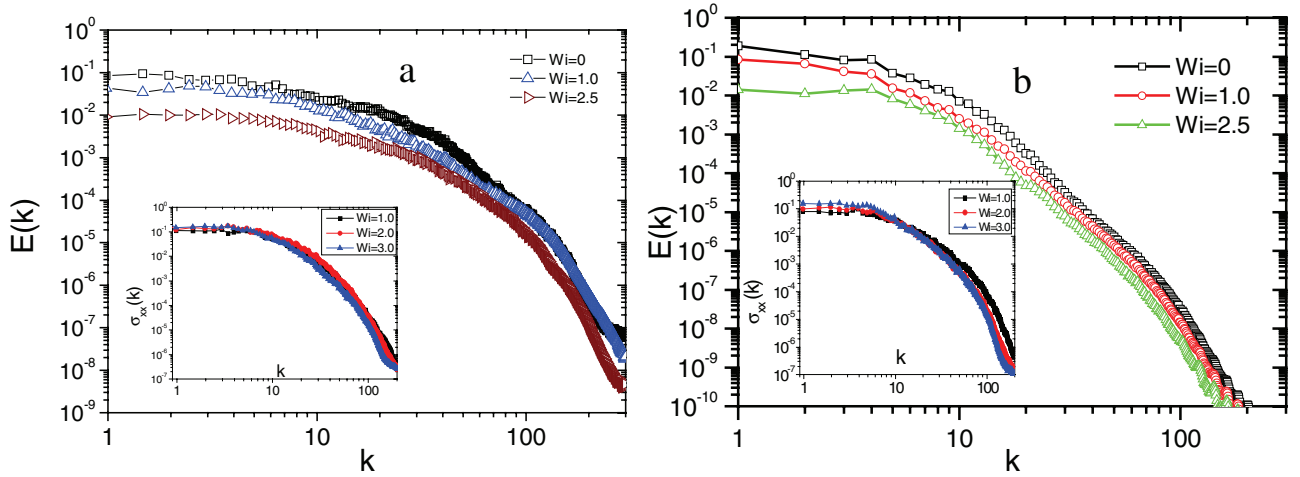


Fig. 3: (Color online) Energy density spectra (calculated from a spatial velocity field) for different Weissenberg numbers and the two configurations used. (a: case 1, b: case 2) For the domain located at  $3 \leq x \leq 4$  and  $0 \leq y \leq 1$ . The insets show the spectra of the longitudinal stress.

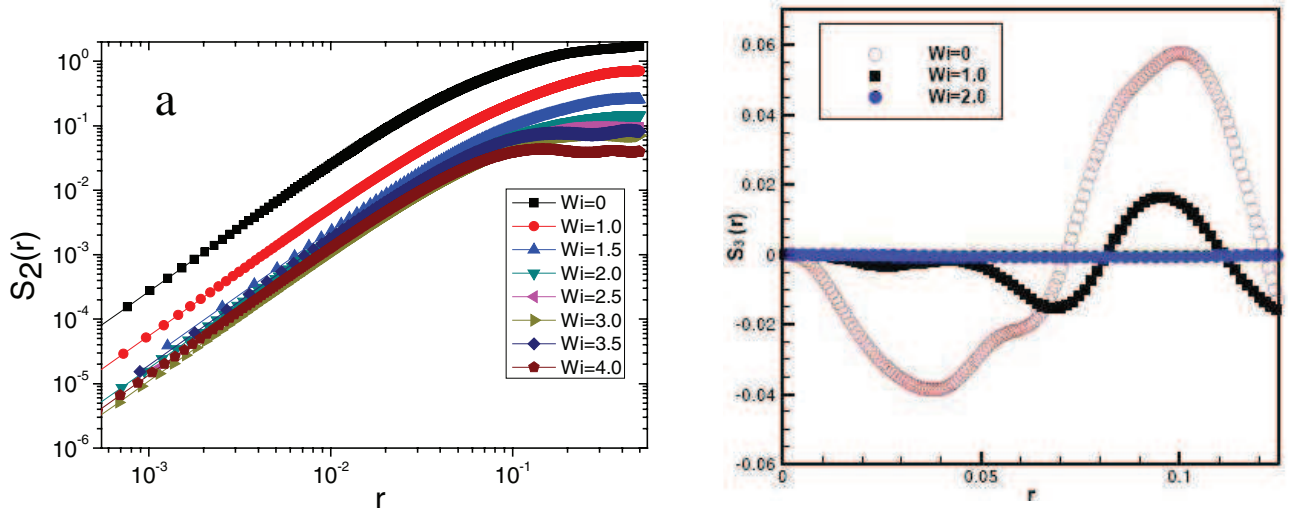


Fig. 4: (Color online) Second and third moment of velocity differences with and without the presence of the polymers at point  $x = 3.8$ ,  $y = 0.4$ .

diagram for the different behaviors in the parameter space described by  $Re$  and  $Wi$  was obtained.

For these simulations, we have examined a large range of Weissenberg numbers. The Reynolds numbers examined ranged from 500 to 10000. This range is close to that usually used in experiments. Two different configurations for the array of cylinders were examined. The first case uses an array of 5 cylinders (denoted case 1) and the second uses an array of 10 cylinders (denoted case 2), increasing the blockage. Most of the analysis presented here focuses on the subdomain  $3 \leq x \leq 4$  for which entrance effects due to the proximity of the cylinders are minimal.

Snapshots of the vorticity field in the channel used are shown in fig. 1 for different  $Wi$ . Note that for increasing

$Wi$ , the wake behind the cylinders has a larger length than for  $Wi = 0$  [14]. Such an increase in length retards the onset of turbulent flow much farther downstream. Note also that the vortex cores are less well defined in the presence of the polymer. A notable feature can be noted for  $Wi = 6$  for which the onset of vortical structures behind the cylinders is so retarded that the existence of vortical structures and turbulence is not observed in the flow domain used. We are not aware of other studies showing that high- $Wi$  flows at high  $Re$  may actually become almost laminar. Another notable feature of these simulations can be appreciated from the variation of the kinetic energy of the velocity fluctuations around the mean ( $\frac{1}{2}u'^2$ ). This energy decreases as the Weissenberg number increases. The mean velocity remains roughly the same

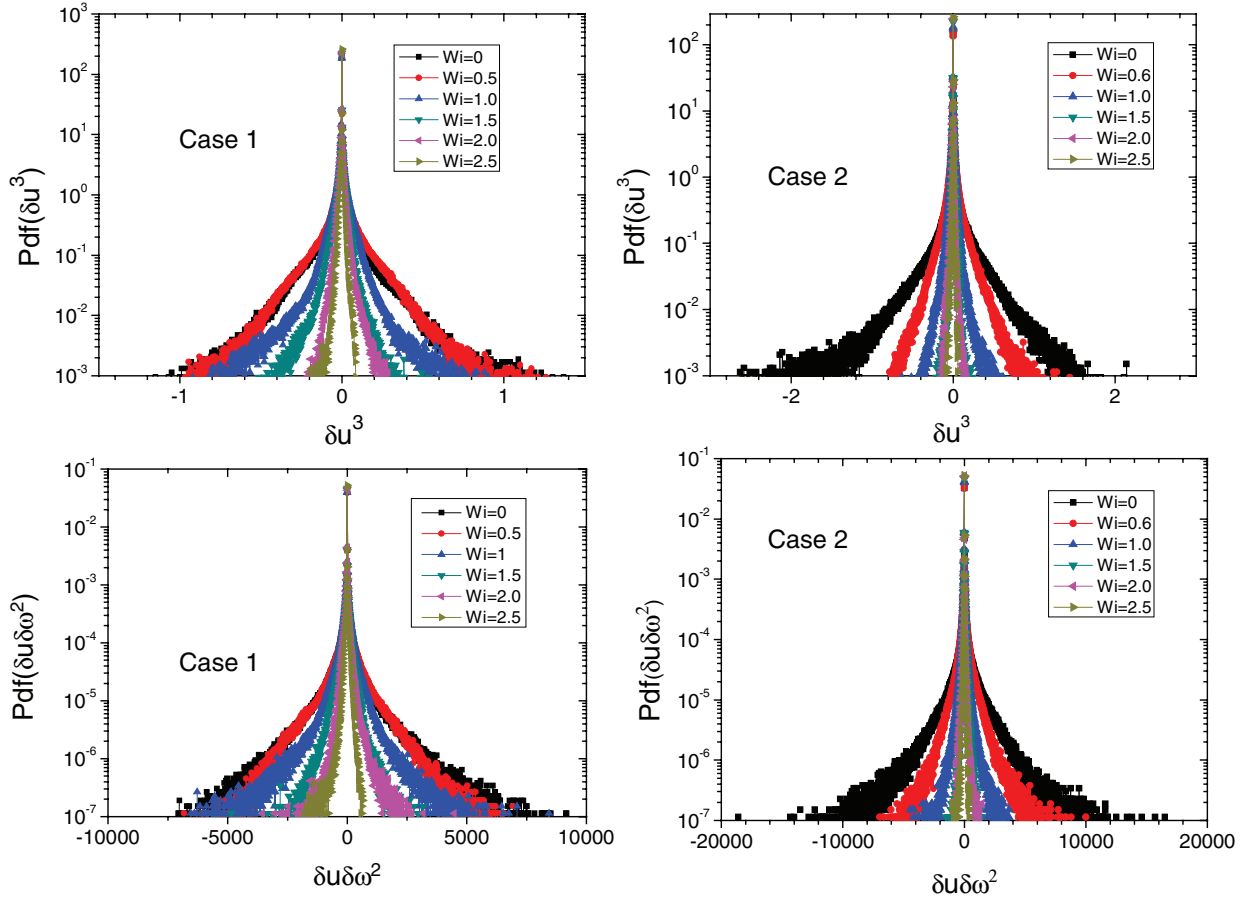


Fig. 5: (Color online) Probability density functions (pdfs) of  $\delta u^3(r)$  and  $\delta u(r)\delta\omega^2(r)$  for different  $Wi$  at  $Re = 5000$  for a separation  $r = R$ . The pdfs were calculated in a spatial window for  $3 < x < 4$  and  $0.25 < y < 0.75$  and for 50 different snapshots of the flow.

for all  $Wi$  and is near 1.2. The reduction of the velocity fluctuations and therefore of the turbulent intensity is shared by the two configurations used as seen in fig. 2. This reduction is, however, much more pronounced for the case with ten cylinders for which the fluctuations are very important near the grid. At the highest  $Wi$  used, the fluctuations become very small due to the fact that the onset of turbulence is retarded and probably occurs much farther downstream than the channel length used here is insufficient (see fig. 1). Also shown in fig. 2 is the elastic energy ( $= 0.5\beta\sigma_{ii}/(Re Wi)$ ). As the kinetic energy of the fluctuations decreases, the elastic energy increases clearly indicating the importance of elastic stresses as  $Wi$  increases at the expense of velocity fluctuations.

The second aspect is revealed by the spectral properties of the fluctuations. Note that in fig. 3(a), the energy density spectra, displayed for different Weissenberg numbers for a Reynolds number of 5000 (case 1), keep roughly the same shape as  $Wi$  increases but that the amplitude at the low wavenumber end or large scales decreases as  $Wi$  increases. This finding mimics experimental results obtained in soap films upon the addition

of polymers in the dilute limit and shows a reduction of the turbulent fluctuations at large scales accompanied by a comparatively smaller reduction at small scales. Figure 3(b) compares spectra for configuration 2 at different  $Wi$ . The first effect noted is a slight reduction of the fluctuations at all scales, somewhat more pronounced than for case 1. By further increasing  $Wi$ , the reduction of the fluctuations is more pronounced at the large-scale end (see fig. 3(b), case 2,  $Re = 5000$ ). Case 1 and case 2 differ somewhat in their suppression of the fluctuations as seen in fig. 2 but for high enough  $Wi$ , the suppression of fluctuations is pronounced at large scales for both cases. The insets of these figures display the corresponding spectra of the elastic stresses. It should be noted that an increase of  $Wi$  results in a reduction of the elastic stresses at small scales but in an increase of these stresses at large scales.

To further examine the effects of the non-Newtonian fluid on the properties of the turbulence, we have examined the second- and third-order structure functions of the longitudinal component of the velocity. The second-order structure function shown in fig. 4(a) shows a similar effect as the energy spectra with a reduction of the amplitude

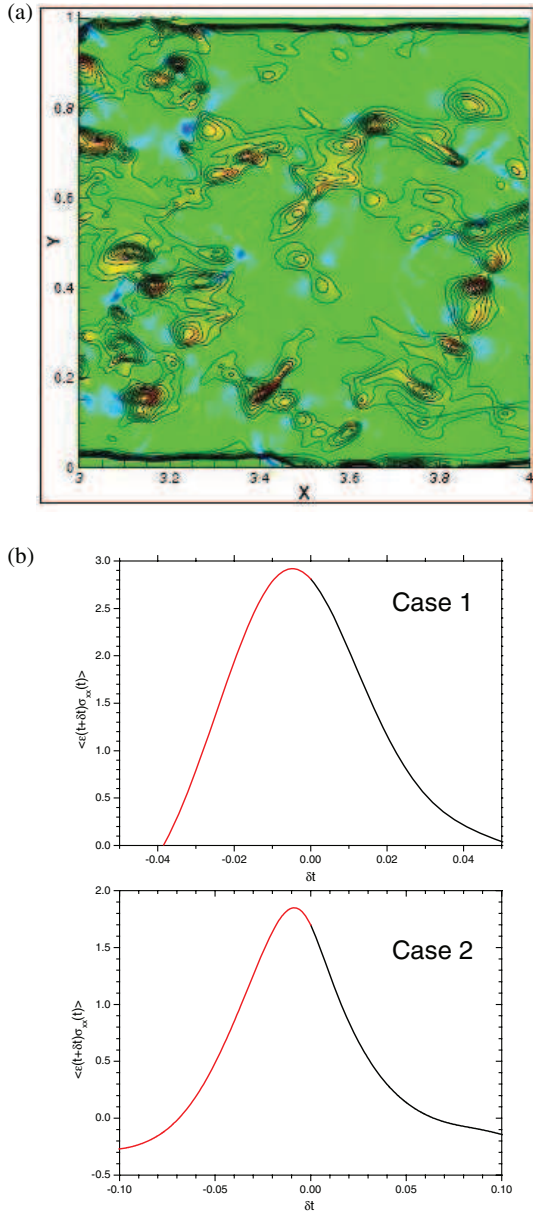


Fig. 6: (Color online) (a) Superposition of elongation (positive elongation is red while negative elongation is blue) and stress contours. Note that the stress increases at locations where the elongation is positive. The domain corresponds to  $3 \leq x \leq 4$  and  $0 \leq y \leq 1$  (b), the elongation stress cross-correlation functions for a single point in the domain  $x = 3.8$ ,  $y = 0.4$ .  $Wi = 1.5$ .

at all scales first followed by a reduction at large scales for higher  $Wi$  shown here for case 2 at  $Re = 5000$ . The third moment is a measure of the energy transfer rate in 2D and 3D turbulence. Figure 4(b) shows that the third moment for the case presented above is positive for the Newtonian case for scales greater than the injection scale which we take to be near the cylinder radius ( $R = 0.025$ ). This moment has a negative dip at smaller scales (near the cylinder radius). Third moments measured

experimentally in turbulent soap films show analogous behavior [4,11,17]. For the non-Newtonian case, the third moment becomes much smaller signaling a reduction in the energy transfer rate as observed experimentally [4]. Since energy is transferred to large scales in 2D turbulence, a reduction of the transfer rate is in agreement with the fact that the energy density of the large scales is smaller than in the Newtonian case. This reduction, however, seems gradual since it is smaller for the intermediate  $Wi$  ( $= 1$ ) than for the higher one ( $= 3$ ).

Besides these features, we have examined the probability density functions (pdfs) of  $\delta u^3(r)$  and  $\delta u(r)\delta\omega^2(r)$ , where  $u$  and  $\omega$  are the longitudinal velocity and the vorticity, respectively. Since in two dimensions, the average of these two quantities is proportional to the spatial scale  $r$  and to the energy transfer rate and the enstrophy transfer rate, respectively [4,18], an examination of the pdfs of these quantities amounts to an examination of the fluctuations of the transfer rates. It turns out that these fluctuations are much less important for the non-Newtonian case. The addition of polymer reduces these fluctuations, as has been found in experiments [4]. One can argue that a reduction of such fluctuations is a sign that elongation rates in turbulence are reduced upon the addition of polymers. In fact, and as fig. 5 shows for representative examples of these pdfs for a separation  $r$  of 1 cylinder radius, both pdfs show a large reduction of large fluctuations. The pdfs of elongation rates confirm directly that large elongations are suppressed upon the addition of polymer as found experimentally.

Now, can these simulations shed more light on this phenomenon? One direct cause of such reduction is the interaction between vortices. In this case the elongation rate  $\epsilon = du/dx$ , and the normal stress  $\sigma_{xx}$  are shown in fig. 6. The first thing that should be noted is that elongation is strongly positive in regions between vortices or just at the edges of vortices. In any case in the region between vortices the flow develops either strong elongation or contraction. The second observation comes from a superposition of the normal stress contours ( $\sigma_{xx}$  is chosen for illustration) and the elongation shown in color in fig. 6(a). Note that the regions of positive elongation are strongly correlated to regions of large normal stresses. Elongation and high stresses therefore coexist at the same locations pointing out that the large positive elongation rates are at the heart of the interaction between the complex fluid and the turbulent flow. Since the large elongations are reduced, one may conclude that the large increase in stresses at locations of high elongation is at the origin of this decrease. In fact, a close examination of the correlation between elongation and normal stresses is shown in fig. 6(b). Here, from a time trace of both signals at a chosen location, it turns out that a large positive peak is obtained for the cross-correlation function  $\langle \epsilon(t+\delta t)\sigma_{xx}(t) \rangle$ . The position of the peak is at a negative time increment  $\delta t$  indicating that elongation increases first before an increase in stress follows. The increase in stress

then must force the elongation to decrease as indicated by the decrease in the correlation function to values near zero and to even negative values showing that the elongation has been turned off to become a contraction.

To conclude, our numerical simulations reproduce several features observed experimentally in two-dimensional turbulence in the presence of polymers. Perhaps the most conspicuous feature is the reduction of large-scale fluctuations associated with the suppression of energy transfers upscale. Besides these observations, the simulations allow for an examination of the stresses in the turbulent flow and the possible links with strong elongations. It turns out that large stresses are present primarily in regions of positive elongation and that when elongation increases in a particular location, the stress starts to increase but with a small lag time. This increase in stress then regulates the increase in elongation. This is one of the keys to the interaction between the polymeric fluid and the flow field. Near the walls of the channel we have also noted a large increase of stresses which may indicate the presence of an elastic layer but this feature needs additional work with higher spatial resolutions near the channel walls. This feature is, however, essential in the understanding of frictional losses in turbulent channel flows.

## REFERENCES

- [1] GYR A. and BEWERSDORFF H. W., *Drag Reduction of Turbulent Flows by Additives* (Kluwer) 1995.
- [2] TABOR M. and DE GENNES P. G., *Europhys. Lett.*, **2** (1986) 519.
- [3] SREENIVASAN K. R. and WHITE C. M., *J. Fluid Mech.*, **409** (2000) 149.
- [4] AMAROUCHENE Y. and KELLAY H., *Phys. Rev. Lett.*, **89** (2002) 104502; KELLAY H., *Phys. Rev. E*, **70** (2004) 036310.
- [5] JUN Y., ZHANG J. and WU X. L., *Phys. Rev. Lett.*, **96** (2006) 024502.
- [6] BOFFETTA G., CELANI A. and MUSACCHIO S., *Phys. Rev. Lett.*, **91** (2003) 034501.
- [7] LVOV V. *et al.*, *Phys. Rev. Lett.*, **92** (2004) 244503; AMAROUCHENE Y. *et al.*, *Phys. Fluids*, **20** (2008) 065108.
- [8] ANGOT P. *et al.*, *Numer. Math.*, **81** (1999) 497.
- [9] SURESHKUMAR R. and BERIS A. N., *J. Non-Newtonian Fluid Mech.*, **60** (1995) 53.
- [10] BRUNEAU C. H. and SAAD M., *Comput. Fluids*, **35** (2006) 326.
- [11] BRUNEAU C. H., GREFFIER O. and KELLAY H., *Phys. Rev. E*, **60** (1999) R1162; KELLAY H., WU X. L. and GOLDBURG W. I., *Phys. Rev. Lett.*, **74** (1995) 3975; **80** (1998) 277; KELLAY H., BRUNEAU C. H. and WU X. L., *Phys. Rev. Lett.*, **84** (2000) 1696; BRUNEAU C. H. and KELLAY H., *Phys. Rev. E*, **71** (2005) 046305.
- [12] TIRTAATMADJA V. and SRIDHAR T., *J. Rheol.*, **39** (1995) 1133.
- [13] BOFFETTA G. *et al.*, *Phys. Rev. E*, **71** (2005) 036307; BERTI S. *et al.*, *Phys. Rev. E*, **77** (2008) 055306.
- [14] XIONG Y. L., BRUNEAU C. H. and KELLAY H., *EPL*, **91** (2010) 64001.
- [15] CRESSMAN J. R., BAILEY Q. and GOLDBURG W. I., *Phys. Fluids*, **13** (2002) 867.
- [16] FRANÇOIS N. *et al.*, *Phys. Rev. Lett.*, **100** (2008) 018302; FRANÇOIS N. *et al.*, *EPL*, **86** (2009) 34002.
- [17] BELMONTE A. *et al.*, *Phys. Fluids*, **11** (1999) 1196.
- [18] KELLAY H. and GOLDBURG W. I., *Rep. Prog. Phys.*, **65** (2002) 1.